J Mol Model (2012) 18:4389–4396
DOI 10.1007/s00894-012-1448-6

ORIGINAL PAPER

Interaction between alkaline earth cations and oxo ligands: a DFT study of the affinity of Mg^{2+} for carbonyl ligands

Leonardo Moreira da Costa · Stanislav R. Stoyanov · José Walkimar de M. Carneiro

Received: 20 March 2012 / Accepted: 23 April 2012 / Published online: 16 May 2012

Abstract The affinities of Mg^{2+} for various substituted carbonyl ligands were determined at the DFT (B3LYP/6-31+G(d)) and semi-empirical (PM6) levels of theory. Two sets of carbonyl ligands were studied: monosubstituted [aldehydes R–CHO and RPh–CHO] and homodisubstituted [ketones R_2C=O and $(RPh)_2C$=O], where R = NH_2, OCH_3, OH, CH_3, H, F, Cl, Br, CN, or NO_2). In the $(RPh)_2CO$ case, the R group was bonded to the *para* position of a phenyl ring. The enthalpies of interaction between the ligands and a pentaaquomagnesium(II) complex were calculated to determine the affinity of each ligand for the Mg^{2+} cation and to correlate with geometrical and electronic parameters. These parameters exhibited the same trends for all of the ligands studied, showing that the affinity of Mg^{2+} for electron-donating ligands is higher than its affinity for electron-withdrawing ligands. In the complexes, electron-donating groups increase both the electrostatic and the covalent components of the Mg–ligand interaction. This behavior correlates with the Mg–O(carbonyl) distance and the ligand electron-donor strength.

Keywords Magnesium cation · Substituent effect · DFT · Interaction enthalpy

Introduction

The interaction between alkaline earth cations and neutral oxo ligands is always a subject of great interest in coordination chemistry, particularly in the fields of biochemistry and catalysis [1, 2]. Divalent magnesium ions (Mg^{2+}) are found ubiquitously throughout the four biological kingdoms, where they have specialized functions [3]. Mg^{2+} is vital for energy production in plant and bacteria cells, as it is an important part of the active structures of chlorophyll and bacteriochlorophyll. In this energy-producing process, sunlight and raw sap are transformed into carbon dioxide, carbohydrates, and oxygen [3]. For eukaryotes, Mg^{2+} is an integral structural component of the DNA and RNA chains that dictate cell biochemistry [4, 5]. In the human body, Mg^{2+} is an important cofactor that interacts with many biological molecules, such as the enzymes that modulate the metabolism of fats and proteins, cell permeability, vascular tone, and neuromuscular excitability [3, 6]. Carbonyl ligands are an important family of Mg^{2+} binding partners in bioinorganic chemistry [3]. The affinity of carbonyl ligands for Mg^{2+} may be understood in terms of Pearson's acid–base theory [7–9], where both the Mg^{2+} cation and the carbonyl group are classified as hard species that tend to form stable complexes with a highly electrostatic component. In pharmaceutical industry, magnesium–carbonyl adducts are widely used as lubricants in the fabrication of tablets and

Electronic supplementary material The online version of this article (doi:10.1007/s00894-012-1448-6) contains supplementary material, which is available to authorized users.

L. Moreira da Costa · J. Walkimar de M. Carneiro (✉)
Programa de Pós-Graduação em Química,
Universidade Federal Fluminense,
Niteroi, Brazil
e-mail: walk@vm.uff.br

S. R. Stoyanov
National Institute for Nanotechnology,
National Research Council of Canada,
11421 Saskatchewan Drive,
Edmonton, Alberta T6G2M9, Canada

J. Walkimar de M. Carneiro
Departamento de Química Inorgânica, Instituto de Química,
Universidade Federal Fluminense,
Outeiro de São João Batista, s/n,
24020-141, Niterói, RJ, Brazil

capsules [10, 11] and as antitumoral (mithramycin), antibacterial (quinolones), ionophore (beauvericin), and antibiotic (valinomycin) drugs [12–14].

Theoretical and experimental studies [15–18] have greatly enhanced our understanding of the interactions between metal cations and ligands. Monofunctional carbonyl, sulfuryl, and phosphoryl ligands were studied by Buncel and Borrajo, who showed, as a general trend, that alkaline earth metal cations interact more strongly with harder (Pearson) bases [15–17]. Yanez et al. published a set of papers analyzing the parameters of biological adducts that affect the strength of binding, such as their specific electron densities, metal oxidation properties, orbital energy distributions, and steric effects [18–22]. A detailed DFT study of the influence of electron donor and electron acceptor groups in a series of *para*-substituted acetophenones on the lithium ion affinity was reported by Senapati et al. [23]. These authors showed that lateral aromatic groups can modulate the interaction strength, which is strongly correlated with some specific electronic and geometrical parameters. Similar trends were found by Palusiak [24] in *para*-substituted $Cr(CO)_5$–pyridine complexes, by Ma [25] in silver complexes with carbonyl, nitrogenous, thio, and aromatic ligands, and by Gal et al. [26] in complexes with substituted phenyl rings. Coordination geometries, electronic features, ion affinities, and binding strengths were analyzed in studies of the interactions of divalent metal cations with aminoacids [27] and nucleosides [28].

In the works cited above, the key point is the interaction between the metal cation and the ligand, which determines the properties of the complexes and modulates the biological effect of each adduct. In the study described in the present paper, as a continuation of our previous investigations on the effects of substituents on the interactions between oxo ligands and alkaline earth cations [29–31], we quantified the binding energies of several carbonyl ligands to a cationic Mg^{2+} pentaaquo complex and analyzed how the neighborhood of the carbonyl group affects these interactions. The interactions between Mg^{2+} and two types of carbonyl ligand—monosubstituted [O=CH(R)] and disubstituted [$O=C(R)_2$] ligands (Fig. 1)—were investigated. The substituents that we analyzed (R = NH_2, OCH_3, OH, CH_3, H, F, Cl, Br, CN, or NO_2) were chosen to simulate the influence of substitution on the carbonyl carbon atom, including resonance and inductive effects [32]. For each series of ligands, there are two patterns of binding: one with the R group directly bonded to the carbonyl carbon atom, and the other with the R group bonded to the *para* position of a phenyl ring. Based on experimental and theoretical studies [33–36] on the coordination number of Mg^{2+} in aqueous media, we considered an Mg^{2+} cation coordinated to six water molecules in an octahedral arrangement and determined the energy required to substitute one of these water molecules for a carbonyl ligand. In addition, geometric, energetic and electronic parameters of the systems that could show correlation with the substitution energy were also evaluated. Donation and backdonation involving the metal–ligand interaction were analyzed using charge decomposition analysis (CDA) [37].

Computational details

DFT calculations were performed with the B3LYP functional [38] and the 6-31+G(d) basis set [39] using the Gaussian 09 software package [40]. It has already been shown that this combination of functional and basis set yields structures that are in good agreement with those obtained at higher levels of theory [18–22, 41, 42]. The semi-empirical calculations were performed with the PM6 method [43] of the MOPAC2009 package [44]. For each ligand, the structures of several conformers obtained by rotation around single bonds were calculated. The structures and energies reported below are for the most stable conformers among the several calculated for each ligand. After full geometry optimization with the B3LYP functional, the second-order force constant matrix was calculated to confirm that the optimized geometry was a genuine minimum on the potential energy surface.

The charge decomposition analysis (CDA) method proposed by Frenking and Dapprich [37] was employed to evaluate the effect of different substituents on the metal–ligand interaction. In this method, the molecule is divided into fragments. The molecular orbitals of the complex are then generated as linear combinations of the fragments' orbitals [45]. In the present work, each adduct $[Mg(H_2O)_5L]^{2+}$ was divided in two fragments: the first was the $[Mg(H_2O)_5]^{2+}$ moiety and the second was the ligand L. In the CDA method, the interaction between fragments is obtained by combining three main terms: (i) the mixing between the occupied orbitals of the first fragment and the empty orbitals of the second fragment, which indicates the electron backdonation; (ii) the mixing between the occupied orbitals of the second fragment and the empty orbitals of the

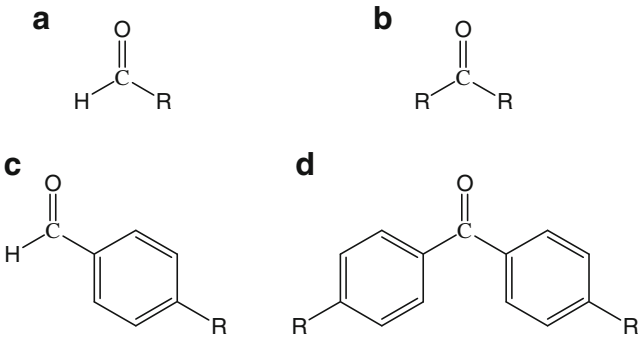

Fig. 1 Structures of the monosubstituted (*a, c*) and disubstituted (*b, d*) carbonyl ligands used for Mg^{2+} complexation

first fragment, which gives the donation; and (iii) the mixing between the occupied orbitals of both fragments, which indicates the charge polarization in the binding region. The CDA calculations were performed with the AOMix 6.55 package [45, 46].

Results and discussion

Geometry optimization

The geometries of the 37 substituted magnesium complexes were fully optimized with the DFT and semi-empirical methods. The optimized geometries for all complexes were similar, with the exception of the distances d_1 (bond length between the Mg^{2+} cation and the carbonyl oxygen atom) and d_2 (C=O double bond) (Fig. 2).

Table 1 lists the B3LYP-optimized distances d_1 and d_2 for each complex. As the Mg^{2+} cation–ligand interaction is predominantly electrostatic in nature [47], the distance between the metal and the ligand (d_1) must reflect its strength. Analysis of Table 1 shows that complexes with electron donor groups have smaller d_1 bond lengths than complexes with electron attractor groups, in agreement with previous theoretical studies [15–22, 28–31]. This behavior confirms that the electronic (inductive and resonance effects) nature of each substituent is correlated with d_1, as reported before [23–25, 29–31]. Electron donation increases the charge on the carbonyl oxygen atom, making the interaction with the magnesium cation stronger, while electron-acceptor groups have the opposite effect. For the monosubstituted complexes, the difference between the strongest electron donor (R = NH_2) and electron-withdrawing substituents (R=NO_2) is 0.07|e| (directly bonded) and 0.03|e| (*para*-substituted), while the difference in charge for the disubstituted complexes is 0.16|e| (directly bonded) and 0.05|e| (*para*-substituted). The bond lengths d_1 for the mono- and disubstituted sets are almost the same. Like d_1, distance d_2 is also correlated with the electronic nature of the substituent. Electron donor groups increase the negative charge on the carbonyl oxygen atom by dislocating the π-electron cloud of the double bond to the carbonyl oxygen atom. This strengths the binding interaction and increases the d_2 distance, whereas electron-acceptor groups pull electron density away from the carbonyl oxygen atom to the double bond, weakening the binding interaction and making the double bond smaller. In summary, the magnesium complexes with electron donor groups have longer d_2 distances than those with electron acceptor groups. Similar results were found by Senapati et al. [23], Ma et al. [25], and in our previous studies [29–31]. The d_2 distances for the mono- and disubstituted sets of ligands are almost the same. The bond lengths d_1 in the magnesium complexes are on average 0.2 Å shorter than those in the analogous Ca^{2+} complexes, mainly due to the difference in the atomic radii of the cations, while d_2 is on average 0.03 Å longer, showing that the binding interaction between carbonyl ligands and the Mg^{2+} cation is stronger. The optimized semi-empirical distances d_1 and d_2 show the same electronic effect dependence (see Table S1 of the "Electronic supplementary material," ESM). This DFT-PM6 trend was previously reported by Puzin et al. [48] and Amin et al. [49].

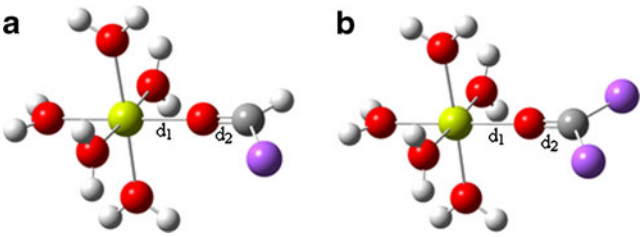

Fig. 2 Structures of the octahedral monosubstituted (*a*) and disubstituted (*b*) magnesium(II) aquocomplexes, showing the distances d_1 (single bond between the Mg^{2+} and the carbonyl oxygen atoms) and d_2 (carbonyl double bond). The Mg^{2+} cation is shown in *yellow*, oxygen atoms are depicted in *red*, and the substituent group R is presented in *purple* in the electronic version of the figure

Interaction enthalpy

The affinity of each ligand for the metal cation was evaluated in terms of the interaction enthalpy, obtained as the heat of reaction (1) corrected to 298 K with the thermal contribution (using unscaled frequencies). The same approach has been used previously to determine the interaction energies between metal cations and ligands [18–31].

$$\left[Mg(H_2O)_6\right]^{2+} + L \leftrightarrows \left[Mg(H_2O)_5L\right]^{2+} + H_2O \qquad (1)$$

Figure 3 shows the correlation between the coordination interaction enthalpy and the value of the Hammett parameter σ_P of the substituent for the *para*-substituted magnesium complexes. Visual inspection shows that complexes with electron-donating groups have more negative interaction enthalpies than those with electron-withdrawing groups. This is due to the resonance structures associated with each group, which modulate the electronic charge on the carbonyl oxygen and control the strength of bonding with the Mg^{2+} cation. This behavior has already been noted for calcium [18–22, 29–31], lithium [23], and chromium [24] cations. In the two series of ligands, the amino-substituted group (R = NH_2) gives the most negative interaction enthalpy, whereas the nitro group (R = NO_2) gives the least exothermic enthalpy. The difference in the binding interaction enthalpies of compounds containing amino and nitro groups is about 24 kcal mol^{-1} for the monosubstituted series and

Table 1 B3LYP/6-31+G(d) interatomic distances d_1 and d_2 (see Fig. 2 for definitions of these distances) in Å, B3LYP and PM6 interaction enthalpies (ΔH) in kcal mol^{-1}, Mulliken charges on the carbonyl oxygen atom (qO, in |e|), Mg atom (qMg, in |e|), and on the whole ligand (qL, in |e|) in pentaaquo Mg^{2+} carbonyl complexes, and the HOMO energy (in hartrees) of the isolated ligand (E_{HOMO})

R group	d_1	d_2	ΔH_{B3LYP}	ΔH_{PM6}	qMg	qO	qL	E_{HOMO}
Monosubstituted ligands								
NH_2	2.02	1.25	−15.45	−20.20	0.903	−0.411	0.277	−0.269
OCH_3	2.06	1.23	−10.54	−18.03	0.899	−0.405	0.267	−0.373
OH	2.07	1.23	−7.02	−15.14	0.896	−0.402	0.264	−0.278
CH_3	2.08	1.23	−3.82	−13.24	0.892	−0.387	0.257	−0.282
H	2.01	1.23	0.49	−6.94	0.890	−0.372	0.252	−0.299
F	2.15	1.21	5.17	−4.24	0.878	−0.349	0.239	−0.331
Cl	2.13	1.22	3.98	−4.97	0.880	−0.358	0.243	−0.326
Br	2.11	1.22	2.53	−5.78	0.884	−0.366	0.246	−0.313
CN	2.15	1.21	7.54	0.16	0.870	−0.338	0.235	−0.346
Ph–NH_2	1.98	1.28	−29.86	−34.53	0.948	−0.442	0.339	−0.224
Ph–OCH_3	2.00	1.27	−24.58	−28.15	0.942	−0.438	0.326	−0.246
Ph–OH	2.00	1.27	−21.73	−26.38	0.938	−0.436	0.324	−0.252
Ph–CH_3	2.01	1.26	−18.51	−22.73	0.932	−0.433	0.319	−0.265
Ph	2.02	1.26	−17.28	−21.13	0.930	−0.430	0.314	−0.269
Ph–F	2.02	1.26	−14.82	−16.87	0.919	−0.424	0.301	−0.274
Ph–Cl	2.02	1.26	−15.33	−17.97	0.924	−0.425	0.306	−0.273
Ph–Br	2.02	1.26	−16.30	−18.84	0.927	−0.427	0.310	−0.268
Ph–CN	2.03	1.25	−7.99	−13.33	0.921	−0.419	0.287	−0.288
Ph–NO_2	2.04	1.25	−5.65	−8.20	0.915	−0.414	0.281	−0.292
Disubstituted Ligands								
NH_2	1.99	1.25	−21.49	−22.08	0.922	−0.426	0.284	−0.269
OCH_3	2.02	1.23	−17.64	−19.35	0.913	−0.418	0.276	−0.298
OH	2.03	1.22	−16.12	−18.24	0.909	−0.415	0.272	−0.319
CH_3	2.04	1.22	−12.74	−14.35	0.899	−0.401	0.264	−0.258
F	2.15	1.20	10.71	−2.06	0.874	−0.327	0.234	−0.377
Cl	2.13	1.20	7.88	−3.61	0.879	−0.332	0.239	−0.334
Br	2.11	1.21	4.14	−5.62	0.891	−0.341	0.242	−0.308
CN	2.15	1.20	15.83	10.43	0.866	−0.317	0.233	−0.367
Ph–NH_2	1.98	1.28	−39.67	−54.88	0.975	−0.466	0.353	−0.216
Ph–OCH_3	1.99	1.27	−34.14	−45.19	0.960	−0.459	0.348	−0.240
Ph–OH	2.00	1.27	−32.29	−42.03	0.953	−0.454	0.342	−0.233
Ph–CH_3	2.00	1.26	−28.83	−38.23	0.948	−0.447	0.330	−0.247
Ph	2.01	1.26	−26.56	−34.54	0.946	−0.439	0.318	−0.255
Ph–F	2.01	1.26	−18.93	−27.00	0.917	−0.418	0.278	−0.263
Ph–Cl	2.01	1.26	−19.85	−27.89	0.920	−0.423	0.294	−0.264
Ph–Br	2.01	1.26	−21.08	−28.66	0.924	−0.428	0.303	−0.261
Ph–CN	2.02	1.25	−6.25	−23.20	0.910	−0.413	0.278	−0.286
Ph–NO_2	2.03	1.25	−3.98	−21.56	0.904	−0.408	0.271	−0.295

35 kcal mol^{-1} for the disubstituted series (Table 1), showing that the inductive and resonance effects of the R group determine the strength of the binding interaction. Table 2 gives the linear fitting parameters for the data shown in Fig. 3. They confirm the interaction enthalpy order given above and, additionally, indicate that the electronic effect of the two R groups in the disubstituted carbonyl compounds leads to an increase in interaction enthalpy of, on average, 7 kcal mol^{-1} [29–31]. The interaction enthalpies computed for the complexes with magnesium are higher than the corresponding ones computed for the complexes with the calcium cation. The smaller cation can better polarize the electronic cloud of the carbonyl oxygen atom, causing a stronger ionic interaction [47]. In general, we found that the interaction enthalpies between the magnesium cation and the carbonyl ligands are about 8 kcal mol^{-1} stronger than those with the calcium cation, in agreement with previous studies [18–22, 27–31].

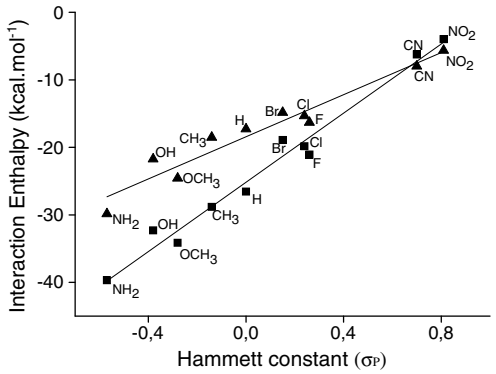

Fig. 3 B3LYP/6-31+G(d) correlation between the coordination interaction enthalpy and the Hammett constant σ_P for the pentaaquo Mg(II) complexes containing monosubstituted (*triangles*) and disubstituted (*squares*) carbonyl ligands

Figures 4 and 5 show graphical representations of the DFT and semi-empirical interaction enthalpies (given in Table 1). Qualitative analysis of the electronic effect of the substituent shows that the semi-empirical method gives the same trends as the DFT method, although with more negative interaction enthalpies, in agreement with previous studies [29–31, 48, 49]. For the monosubstituted complexes, the PM6 enthalpies are on average 7.9 (±1.4) kcal mol^{-1} (directly bonded) and 3.6 (±1.1) kcal mol^{-1} (*para*-substituted) more negative than the DFT values, whereas for the disubstituted complexes the differences are on average 5.7 (±4.6) kcal mol^{-1} (directly bonded) and 11.2 (±3.2) kcal mol^{-1} (*para*-substituted). The PM6 Ca^{2+}–carbonyl interaction enthalpies [29–31] are about 10 kcal mol^{-1} lower than the corresponding Mg^{2+}–carbonyl interaction enthalpies, in good accord with the DFT results. This shows that the magnesium and calcium parametrizations of the PM6 method are in agreement with the DFT calculation, indicating that this semi-empirical method can be used for the qualitative analysis of divalent cation (Mg^{2+}, Ca^{2+})–ligand interactions.

Considering that the electrostatic component is predominant [18–22, 29–31, 47], the charges on the atoms involved in the binding interaction are important determinants of its strength. As discussed in the "Geometry optimization" subsection, the cases where the interaction occurs between atoms with the largest charge differences are also those that have the highest coordination interaction enthalpies. In Table 1, we list the charges on the Mg and O (carbonyl) atoms calculated using the Mulliken population analysis method and the B3LYP functional. Analysis of these charges shows a common trend [27–31] where complexes with electron-donating groups have higher charges on the atoms that participate in the interaction than complexes with electron-withdrawing groups. The difference between the charges on the magnesium and carbonyl oxygen atoms confirms that the interaction is stronger in complexes with electron donor groups, in agreement with the geometry and enthalpy results discussed above (Table 1).

Charge decomposition analysis

The interaction between Pearson hard acids and bases is predominantly electrostatic. However, it may also have a certain degree of covalent character due to the overlap of atomic orbitals and charge polarization [47]. A donor–acceptor charge polarization process can be quantified via the CDA approach [37]. The CDA method calculates both the electron donation and the backdonation, and from them, the amount of charge transfer. For the systems studied here, as Mg^{2+} does not have any high-energy occupied *d* orbitals available, the backdonation should be negligible (see Table S2 of the ESM). This is confirmed by the CDA results, and follows previous studies [18–22, 29–31]. The charge transfer from the $[Ca(H_2O)_5]^{2+}$ fragment to the ligand is close to zero, even in the case of the strongly electron-attracting substituents [18–22]. Therefore, the charge transfer process is dictated solely by the donation from the ligand to the cation aquocomplex, in agreement with previous studies [18–22, 25, 27, 29–31]. Figure 6 shows the correlation between the interaction enthalpy and the charge donation calculated using the CDA approach for the *para*-substituted compounds. As can be seen, there is a high correlation between these two properties (r^2=0.96 for the monosubstituted compounds and r^2=0.95 for the disubstituted ones). Complexes with electron donor groups have higher CDA donation than the corresponding compounds with electron-withdrawing groups. The amino–nitro difference in the CDA donation for the monosubstituted compounds is 0.060|e|, while it is 0.095|e| for the disubstituted ones. These results show that electron donation from the ligand to the cation also strengthens the ligand–metal binding, even if the interaction is predominantly electrostatic. The CDA donation from carbonyl ligands to the magnesium aquocenter is on average 0.200|e| higher than that to the calcium aquocomplex, meaning that the binding interaction with Mg^{2+} is stronger than that with Ca^{2+} [29–31]. This can be understood by considering two effects. First, the size of the carbonyl oxygen atom is closer to the size of the magnesium atom, thus facilitating the orbital overlap and strengthening the covalent interaction, than to the size of the calcium atom [47]. Second, as Mg^{2+} is smaller than

Table 2 Linear fitting analysis for the data shown in Fig. 3

	Intercept (kcal mol^{-1})	Slope (kcal mol^{-1})	R^2
Monosubstituted	−18.44	15.59	0.93
Disubstituted	−25.18	25.62	0.98

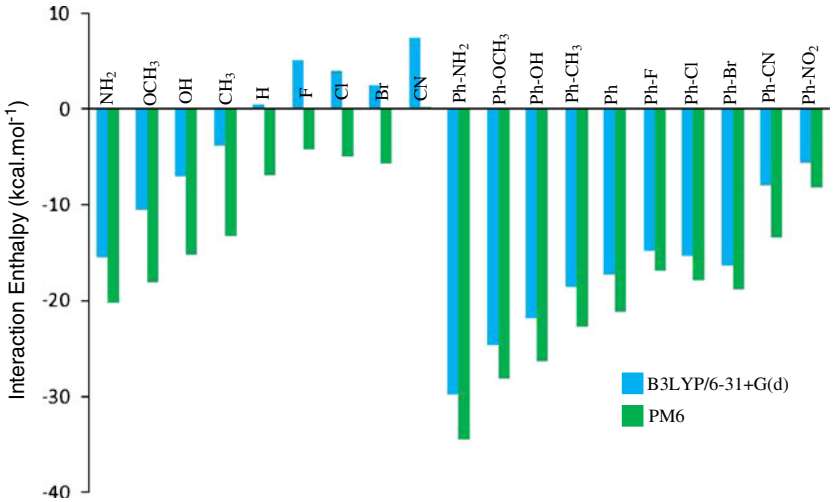

Fig. 4 Coordination interaction enthalpies calculated according to Eq. 1, using the B3LYP/6-31 +G(d) and the PM6 methods, for the pentaaquo Mg(II) complexes containing monosubstituted carbonyl ligands

Ca^{2+}, it polarizes the ligand more strongly and increases the covalent charge donation due to charge polarization [47].

The charge transfer from the ligand to the metal cation can also be quantified by the charge on the ligand after the complexation process. In Table 1, we list the charges on the ligand after complexation with the metal cation. As expected, species with electron donor groups are able to transfer a great deal of the charge density to the metal center, thus following the same trend as seen in the analyses of the distances and atomic charges. The charge on the ligand in the disubstituted complexes are on average 0.02|e| higher than the charge on the ligand in the monosubstituted compounds, confirming that the covalent component does not change much along a series with the same metal cation. These trends were also found by Senapati et al. [23] and Ma et al. [24].

The correlations given above clearly indicate that the ability of the ligand to transfer charge density to the metal center is an important parameter determining the coordination interaction enthalpy. When analyzed from the point of view of the interaction between two fragments, charge transfer should be associated with the HOMO–LUMO energy difference between the two fragments. In the present case, the accepting fragment $[Mg(H_2O)_5]^{2+}$ is constant, so the important factor is the HOMO energy of the ligand. It is expected that ligands with higher HOMO energies are better electron donors, while those with lower HOMO energies are poorer electron donors. The values of the HOMO energies of the ligands are also listed in Table 1. Ligands with electron-donating groups have higher HOMO energies than those with electron-withdrawing groups [50, 51]. Therefore, they are more prone to donating electrons than electron-withdrawing groups are. This also correlates with the strength of the metal–ligand binding.

Conclusions

The ability of carbonyl ligands to complex the Mg^{2+} cation was analyzed in terms of geometric (distance between the cation and the ligand, and the carbonyl double bond), energetic (coordination interaction enthalpy), and electronic (charge donation and backdonation, and charges on the magnesium cation, the carbonyl oxygen atom, and the whole ligand)

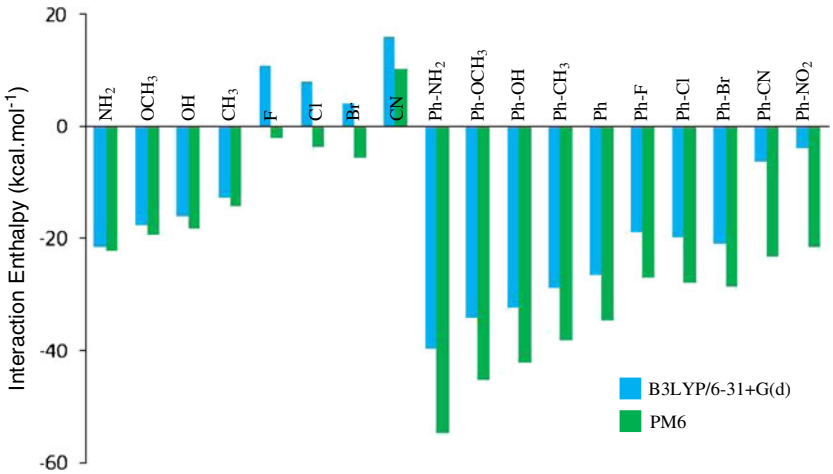

Fig. 5 Coordination interaction enthalpies calculated according to Eq. 1, using the B3LYP/6-31 +G(d) and the PM6 methods, for the pentaaquo Mg(II) complexes containing disubstituted carbonyl ligands

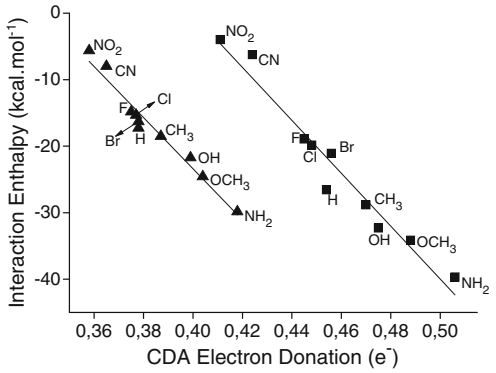

Fig. 6 The B3LYP/6-31+G(d) correlation between the coordination interaction enthalpy and CDA electron donation for the pentaaquo Mg (II) complexes containing *para*-monosubstituted (*triangles*) and *para*-disubstituted (*squares*) carbonyl ligands

properties. We studied 19 ligands with monosubstituted [O=C(H)R] and 18 with disubstituted [$O=C(R)_2$] carbonyl groups. Electron-donating substituents were found to strengthen the ligand–cation interaction, leading to a more exothermic interaction enthalpy, while electron-withdrawing substituents were observed to have the opposite effect. Electron-donating groups strengthen the cation–ligand interaction by increasing both its electrostatic and covalent components. The electrostatic component was found to correlate with the cation–ligand bond length (d_1) and the charges of the atoms that participate in the interaction. Electron-donating groups increase the negative charge on the carbonyl oxygen atom and reduce the distance d_1, thereby strengthening the ionic component of the interaction. The covalent component of the interaction was observed to correlate with the CDA electron donation from the ligand to the metal center and also with the charge transfer from the ligand after complexation. In both cases, we found that electron-donating groups increase the ligand-to-metal charge transfer, strengthening the covalent component of the interaction. The HOMO energy of the ligand is another parameter that correlates with the coordination interaction enthalpy. Electron donor ligands have higher HOMO energies than electron-withdrawing ligands. The B3LYP/6-31+G(d) and PM6 methods give qualitatively the same trends for the variation in the interaction enthalpy with respect to the Hammett parameter σ_P. Quantitatively, the interaction enthalpies calculated with the PM6 method are more negative than those obtained with the B3LYP/6-31+G(d) method.

Acknowledgments J.W. de M. Carneiro has a research fellowship from Conselho Nacional de Desenvolvimento Científico (CNPq). L.M. da Costa has a graduate fellowship from CAPES (Coordenadoria de Aperfeiçoamento de Pessoal de Nível Superior). Financial support from FAPERJ (Fundação Carlos Chagas Filho de Amparo a Pesquisa do Estado do Rio de Janeiro) is also kindly acknowledged. S.R. Stoyanov acknowledges the financial support of the Imperial Oil–Alberta Ingenuity Centre for Oil Sands Innovation (COSI) at the University of Alberta in Edmonton, Alberta, Canada and the National Institute for Nanotechnology (NINT), a joint initiative of the National Research Council of Canada, the University of Alberta, the Government of Alberta, and the Government of Canada.

References

1. Poonia NS, Bajaj AV (1979) Chem Rev 79:389–445
2. Daniele PG, Foti C, Gianguzza A, Prenesti E, Sammartano S (2008) Coord Chem Rev 252:1093–1107
3. Maguire ME, Cowan JA (2008) Biometals 15:203–210
4. Romani AMP, Maguire ME (2008) Biometals 15:271–283
5. Owczarzy R, Moreira BG, You Y, Behlke MA, Walder JA (2008) Biochemistry 47:5336–5353
6. Sreedhara A, Cowan JA (2008) Biometals 15:211–223
7. Pearson RG (1963) J Am Chem Soc 85:3533–3543
8. Pearson RG (1966) Science 151:172–177
9. Pearson RG, Songstad J (1967) J Am Chem Soc 89:1827–1836
10. Uchimoto T, Iwao Y, Takahashi K, Tanaka S, Agata Y, Iwamura T, Miyagishima A, Itai S (2011) Eur J Pharm Biopharm 78:492–498
11. Barra J, Somma R (1996) Drug Dev Ind Pharm 22:1105–1120
12. Bergen WG, Bates DB (1984) J Ani Sci 58:1465–1483
13. Choi HJ, Lee DH, Park YS, Lee IK, Kim YC (2002) J Incl Pheno Macrocy Chem 43:15–18
14. Wallace RJ (1994) J Anim Sci 72:2992–3003
15. Buncel E, Decouzon M, Formento A, Gal JF, Herreros M, Li L, Maria PC, Koppel IA, Kurg R (1997) J Am Soc Mass Spectrom 8:262–269
16. Borrajo AMP, Gal JF, Maria PC, Decouzon M, Ripley DC, Buncel E, Thatcher GRJ (1997) J Org Chem 62:9203–9209
17. Buncel E, Chen A, Decouzon M, Fancy SA, Gal JF, Herreros M, Maria PC (1998) J Mass Spectrom 33:757–765
18. Corral I, Mó O, Yáñez M, Scott AP, Radom L (2003) J Phys Chem A 107:10456–10461
19. Trujillo C, Lamsabhi AM, Mó O, Yánez M, Salpin (2008) J Org Biomol Chem 6:3695–3702
20. Corral I, Mó O, Yánez M, Salpin J, Tortojada J, Moran D, Radom L (2006) Chem Eur J 12:6787–6796
21. Corral I, Mó O, Yánez M, Salpin J, Tortojada J, Radom L (2004) J Phys Chem A 108:10080–10088
22. Trujillo C, Lamshabi AM, Mó O, Yánez M (2008) Phys Chem Chem Phys 10:3229–3235
23. Senapati U, De D, De BR (2007) J Mol Struct (THEOCHEM) 808:157–159
24. Palusiak M (2007) J Organomet Chem 692:3866–3873
25. Ma NL (1998) Chem Phys Lett 297:230–238
26. Gal JF, Maria PC, Decouzon M, Mo O, Yanez M (2002) Int J Mass Spectrom 219:445–456
27. Tehrani ZA, Fattahi A, Pourjavadi A (2009) J Mol Struct (THEOCHEM) 913:117–125
28. Tavasoli E, Fattahi A (2009) J Theor Comput Chem 8:347–371
29. Costa LM, Carneiro JWM, Paes LWC, Romeiro GA (2009) J Mol Struct (THEOCHEM) 911:46–51
30. Costa LM, Carneiro JWM, Paes LWC, Romeiro GA (2011) J Mol Model 17:243–249
31. Costa LM, Carneiro JWM, Paes LWC (2011) J Mol Model 17:2061–2067
32. Krygowski TM, Stepién BT (2005) Chem Rev 105:3482–3512
33. Dudev M, Wang J, Dudev T, Lim C (2006) J Phys Chem B 110:1889–1895
34. Tunell I, Lim C (2006) Inorg Chem 45:4811–4819
35. Rao JS, Dinadayalane TC, Leszczynski J, Sastry GN (2008) J Phys Chem A 112:12944–12953
36. Adrian-Scotto M, Mallet G, Vasilescu D (2005) J Mol Struct (THEOCHEM) 728:231–242
37. Dapprich S, Frenking G (1995) J Phys Chem 99:9352–9362

38. Becke AD (1992) J Chem Phys 96:2155–2160
39. Rassolov VA, Ratner MA, Pople JA, Redfern PC, Curtis LA (2001) J Comput Chem 22:976–984
40. Frisch MJ, Trucks GW, Schlegel HB, Scuseria GE, Robb MA, Cheeseman JR, Scalmani G, Barone V, Mennucci B, Petersson GA, Nakatsuji H, Caricato M, Li X, Hratchian HP, Izmaylov AF, Bloino J, Zheng G, Sonnenberg JL, Hada M, Ehara M, Toyota K, Fukuda R, Hasegawa J, Ishida M, Nakajima T, Honda Y, Kitao O, Nakai H, Vreven T, Montgomery JA Jr, Peralta JE, Ogliaro F, Bearpark M, Heyd JJ, Brothers E, Kudin KN, Staroverov VN, Kobayashi R, Normand J, Raghavachari K, Rendell A, Burant JC, Iyengar SS, Tomasi J, Cossi M, Rega N, Millam NJ, Klene M, Knox JE, Cross JB, Bakken V, Adamo C, Jaramillo J, Gomperts R, Stratmann RE, Yazyev O, Austin AJ, Cammi R, Pomelli C, Ochterski JW, Martin RL, Morokuma K, Zakrzewski VG, Voth GA, Salvador P, Dannenberg JJ, Dapprich S, Daniels AD, Farkas Ö, Foresman JB, Ortiz JV, Cioslowski J, Fox DJ (2009) Gaussian 09, revision A.1. Gaussian Inc., Wallingford
41. Prado MAS, Garcia S, Martins JBL (2006) Chem Phys Lett 418:264–267
42. Abirami S, Ma NL, Goh NK (2002) Chem Phys Lett 359:500–506
43. Stewart JJP (2007) J Mol Model 13:1173–1213
44. Stewart JJP (2009) MOPAC 2009, version 11.038 W. Stewart Computational Chemistry, Colorado Springs
45. Gorelsky SI, Lever ABP (2001) J Organomet Chem 635:187–196
46. Gorelsky SI (2007) AOMix: program for molecular orbital analysis. University of Ottawa, Ottawa
47. Huheey JE, Keiter EA, Keiter RL (1993) Inorganic chemistry: principles of structure and reactivity, 4th edn. HarperCollins, New York
48. Puzin T, Suzuki N, Haranczyk M, Rak J (2008) J Chem Inf Model 48:1174
49. Amin EA, Truhlar DG (2008) J Chem Theor Comput 4:75–85
50. Sizova O, Varshavskii Y, Skripnikov L (2007) Russ J Coord Chem 33:313–322
51. Fragoso TP, Carneiro JWM, Vargas MD (2010) J Mol Model 16:825–830